Nuclear Physics with Antiprotons

T. von Egidy[a], F. J. Hartmann[a], S. Schmid[a], W. Schmid[a], K. Gulda[b], J. Jastrzebski[b], W. Kurcewicz[b], P. Lubinski[b], L. Pienkowski[b], A. Trzcinska[b], D. Hilscher[c], W. Bohne[c], F. Goldenbaum[c], U. Jahnke[c], D. Polster[c], H. Rossner[c], A. S. Iljinov[d], D. I. Ivanov[d], M. V. Mebel[d], V. G. Nedorezov[d], A. S. Sudov[d], J. Eades[e], and S. Neumaier[e]

[a] Physik-Department, Technische Universität München, D-85748 Garching, Germany
[b] Warsaw University, PL-02-097 Warsaw, Poland
[c] Hahn-Meitner-Institut, D-14109 Berlin, Germany
[d] Institute of Nuclear Research, Russian Academy of Sciences, 117312 Moscow, Russia
[e] CERN, CH-1211 Geneva 23, Switzerland

Z. Naturforsch. **50a,** 1077–1082 (1995); received October 2, 1995

Information on the neutron distribution in the nuclear periphery was obtained by the annihilation of stopped antiprotons and the yield of residual nuclei. The last atomic transitions of the antiproton before annihilation gives complementary results. Properties of very hot nuclei (up to 1 GeV) after annihilation of stopped antiprotons were studied by neutron emission and fission. Absolute probabilities of fission induced by stopped and fast antiprotons were determined. The experimental data are compared with elaborate calculations taking into account the annihilation process, the fast cascade and pre-equilibrium emission, thermalisation, particle evaporation and fission.

1. Introduction

The interaction of antiprotons and nuclei yields a wealth of new and interesting information on atomic nuclei [1]. Stopped antiprotons form antiprotonic atoms and cascade down to lower orbits by emission of of x-rays and Auger electrons. As soon as the antiproton touches the nuclear surface, it annihilates with a proton or neutron. This happens already at more than twice the nuclear radius, where the nuclear density is only a few percent of the central density. The last populated orbit has principal quantum numbers $n=5$ for Ni and $n=9$ for U. Consequently, careful analysis of experimental observations may yield information on the neutron and proton densities at these distances. One method is the measurement of the last antiprotonic x-rays, their widths, shifts and intensities. This has been done with sufficient precision only for few nuclides. But a new series of such measurements began in 1995 at LEAR/CERN (PS 209). Another method was developed recently by our group (PS 203) [2, 3]. It uses the yield of $(N-1)$ and $(Z-1)$ nuclei after antiproton annihilation (N and Z are neutron and proton numbers of the target, respectively). This yield reflects the neutron and proton densities at large distances as will be discussed later.

Reprint requests to Prof. T. von Egidy.

The antiproton annihilation produces between 2 and 8 pions with mean energies of several hundred MeV (and in a few percent of the annihilations also kaons). Some of these particles enter the nucleus and heat it to thermal energies up to nearly 1 GeV. In contrast to heavy ion collisions this multipion reaction has a relatively smooth energy transfer without compression or large angular momentum. Therefore, reactions in very hot nuclei may differ from those produced otherwise. We studied particle emission, distribution of residual nuclei and fission, and obtained information in a series of target nuclides on processes in very hot nuclei, distributions of thermal excitation energies, the time scale of these processes and fission probabilities.

In order to understand all these reactions, detailed Monte Carlo calculations were performed which simulate all steps of processes, the antiprotonic atom, the fast intranuclear cascade, coalescence emission of particles, pre-equilibrium stages, evaporation, fission and evaporation from fragments. This resulted in a good overall reproduction of the experimental data in many cases.

2. Study of the Nuclear Periphery with Antiprotons

In about 10% of all cases when an antiproton annihilates with a heavier nucleus, almost no excitation

0932-0784 / 95 / 1100-1077 $ 06.00 © – Verlag der Zeitschrift für Naturforschung, D-72027 Tübingen

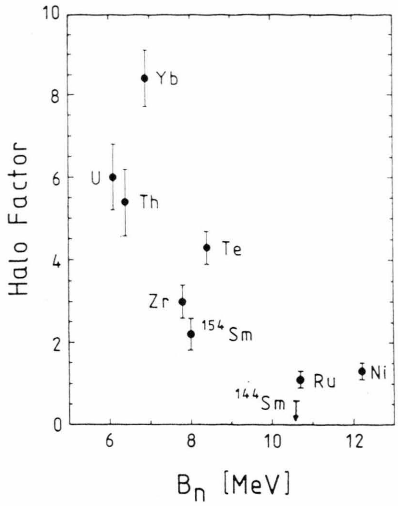

Fig. 1. Neutron halo factor plotted as a function of the neutron binding energy B_n [3].

energy is transfered to the nucleus, either because the annihilation takes place too far outside the nucleus, or because too few pions are produced. Consequently, residual nuclei are obtained with only one neutron or one proton missing from the annihilation. The number of these $(N-1)$- and $(Z-1)$-nuclei is proportional to the density of neutrons and protons in the far periphery of the nucleus, respectively. The numbers can be determined experimentally by measuring the γ-activity of the $(N-1)$- and $(Z-1)$-nuclei. This has been done by our group for a series of target nuclides between Ni and U and shows that in about 10% of all annihilations in heavier nuclei only $(A-1)$-nuclei are produced [4]. Only ^{130}Te and ^{176}Yb have larger values, which can be explained with the E2 resonance effect [5]. A neutron halo factor can be defined which gives the ratio of the neutron density to the proton density in the far periphery of the nucleus, corrected for the N/Z ratio and the antiproton absorption probability ratio at neutrons and protons [3].

This halo factor is displayed in Figure 1. A strong dependence on the neutron binding energy B_n is observed, indicating the obvious fact that loosely bound neutrons have larger radii and present some kind of halo. The theoretical interpretation of these results is in progress.

The width, energy shift and yield of antiprotonic x-rays also give information on the neutron density in the nuclear periphery. The combined evaluation of both mentioned methods is expected to improve our knowledge in this field. First experiments this year seem to indicate a strong change of the last antipro-

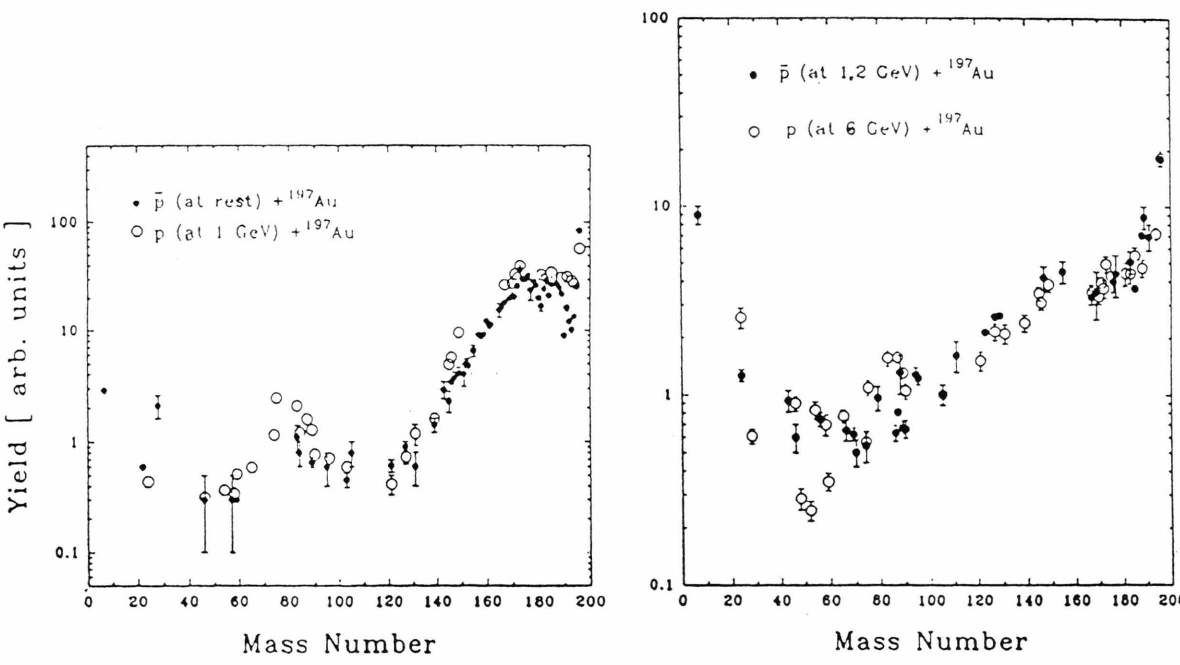

Fig. 2. Distribution of residual nuclei after interaction of stopped antiprotons and 1 GeV protons (left side) and 1.2 GeV antiprotons and 6 GeV protons (right side) with Au targets.

tonic x-ray intensities of the isotopes between ^{58}Ni and ^{64}Ni, probably due to the increasing radius of the neutron distribution.

3. Residual Nuclei After Antiproton Absorption

The number of emitted particles after antiproton annihilation in heavier nuclei is roughly proportional to the thermal excitation energy. Since mass losses up to 80 nucleons were observed after the annihilation of stopped antiprotons in U, excitation energies of 700 MeV can be achieved [6]. It is an interesting question whether the distribution of excitation energies obtained by antiproton annihilation is basically different from excitations with other projectiles. We give here the example of ^{197}Au targets bombarded with stopped and 1.2 GeV antiprotons [7] and with 1 GeV and 6 GeV protons [8]. The distribution of residual nuclei was measured by their induced γ activity. Figure 2 shows that the mass loss and consequently the excitation energy is very similar for the corresponding reactions and therefore indicates similar heating mechanisms. However, antiprotons bring much more thermal energy into the nucleus with less projectile energy.

4. Neutron Emission Before and After Scission of U Targets

It has been shown recently that the time scale of processes in very hot nuclei can be investigated by measuring the number of neutrons emitted before and after scission [9, 10]. Our experimental arrangement is shown in Figure 3. We measured the time-of-flight neutron spectra emitted parallel and perpendicularly to the fission axis following antiproton annihilation in ^{238}U. These spectra can be decomposed by a moving-source-fit into five Maxwellian-like distributions originating namely from the fast intranuclear cascade (INC) (10^{-22} s), pre-equilibrium emission (PE) (10^{-21} s), evaporation from the compound nucleus before scission (CN) (10^{-20} s) and evaporation from fission fragments parallel, antiparallel or 90° to the fragments (FF) (10^{-18} s). This is shown in Fig. 4 (upper part). Table 1 gives the obtained neutron multiplicities and T-parameters for the various stages of the hot nucleus. A more detailed analysis of these multiplicities and T-parameters as a function of the mass loss (determined by E_{kin} and time-of-flight of the fission fragments) shows that the multiplicities of the neutron spectra before scission increase with the mass loss (excitation energy) while the neutron multiplicities from the fragments and all T-parameters are rather independent of the mass loss.

The neutron multiplicity after scission is in good agreement with results from heavy ion reaction (Table 2), which demonstrates that fission is in most cases a rather slow process giving the nucleus enough time to cool until it reaches the scission point [9, 10]. An increase of the excitation energy mainly increases the pre-scission neutron numbers. However, the theoretical calculations with the intranuclear cascade evaporation model [14] show a strong dependence of the evaporation spectra from fission fragments on the

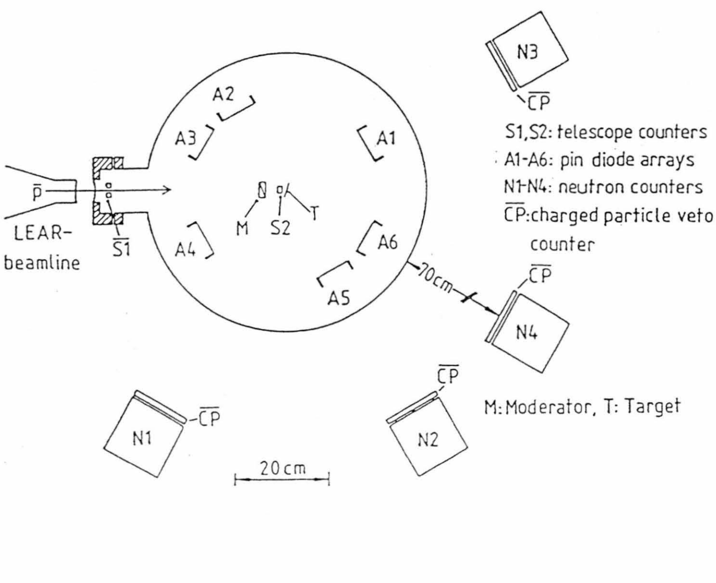

Fig. 3. Experimental arrangement to measure particle spectra in coincidence with both fission fragments.

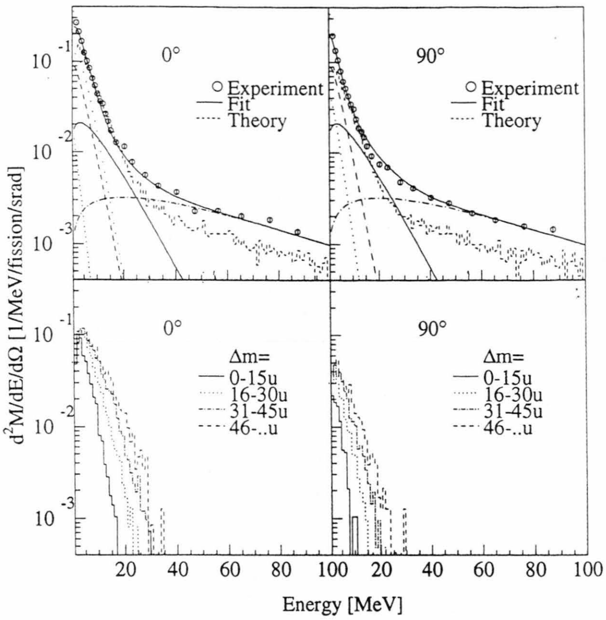

Fig. 4. Neutron spectra emitted after antiproton annihilation in ^{238}U at 0° and 90° to the fission axis. The upper part shows the experimental spectra with the decomposition in the INC (dot-dash), PE (full line), CN (large dashes) and FF (dot) components. The calculated spectra have small dashes. The lower part displays calculated spectra of post-scission neutrons (FF) for different mass loss (excitation energy) windows.

mass loss (lower part of Figure 4). The total calculated neutrons spectrum is shown in the upper part of Fig. 4 (small dashes). The calculated spectrum above 30 MeV is about a factor 2 smaller than the measured spectrum. This is a serious deficiency of the theory which was observed already earlier and cannot be resolved easily.

Table 1. Neutron multiplicities and T-parameters of Maxwellian distributions of the different neutron emission stages in a U target.

	INC	PE	CN	FF
Multiplicity per fission	3.3 (3)	4.1 (4)	6.2 (6)	3.2 (3) × 2
T-parameter in MeV	40 (4)	7.5 (5)	2.6 (2)	1.9 (2)

Table 2. Pre- and post-scission neutron multiplicities from different reactions.

Reaction	E*/MeV	M (PE+CN)	M (FF)	Ref.
$^{20}Ne+^{209}Bi$	120	5.7 (4)	6.4 (5)	[11]
$p+^{238}U$	140	8.4 (17)	8.6 (17)	[12]
$^{16}O+^{208}Pb$	187	7.8 (3)	6.8 (3)	[13]
$\bar{p}+^{238}U$	220	10.3 (7)	6.3 (6)	this work

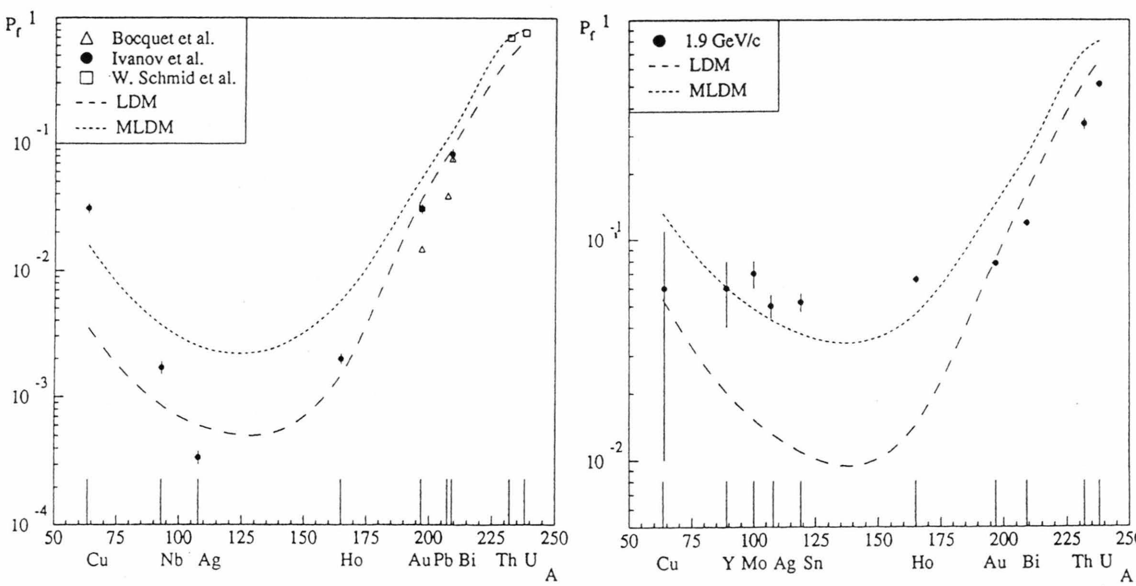

Fig. 5. Absolute probabilities of antiproton induced fission as a function of A. The data with triangle are from Bocquet et al. [19]. The curves are calculated with the liquid drop model (LDM) and the modified liquid drop model (MLDM). The left side shows the values for stopped antiprotons and the right side the values for 1.2 GeV antiprotons.

5. Probability of Fission Induced by Stopped and Fast Antiprotons

Fission probabilities provide information on fission barriers, but how the fission barrier depends on the excitation energy is still an open problem. This question is related to the surface tension and viscosity as a function of temperature in nuclear matter. Since antiproton annihilation is a very special way to obtain very hot nuclei, it is desirable to study fission probabilities as a function of the target mass number. Theoretical calculations are available and predict a minimum near Ag. We determined recently with a special wire chamber and also with pin diodes the probability of fission induced by stopped antiprotons for a series of targets between Cu and U (Fig. 5, left side) [15, 16]. The minimum near Ag is clearly visible. With the new 4π neutron and 4π charged-particle detector, the Berlin Ball (PS 208) [17, 18], we measured fission probabilities for 1.2 GeV antiprotons (Fig. 5, right side). Due to the higher excitation energy and the resulting larger mass loss the minimum near Ag disappeared. However, fission events are not easy to identify and to separate from multifragmentation in light nuclei. The values below Ag have to be considered, therefore, to be to some extent upper limits. Figure 5 shows that neither the calculations with the liquid drop model (LDM) nor with the modified liquid drop model (MLDM) [20] are able to reproduce all data with stopped or 1.2 GeV antiprotons. A new effort is necessary to understand fission of hot nuclei and nuclei with lower A.

6. Conclusion

Antiprotons are a very valuable probe for investigating nuclei under special conditions. Antiprotonic atoms and stopped antiproton annihilation with nearly no energy transfer both give information on the neutron density in the nuclear periphery. Particle emission and residual nuclei distributions provide insight into processes in very hot nuclei. Fission studies elucidate the time scale of the processes and are related to the fission barrier in hot nuclei. Concerning the $\bar{p}$-induced fission we have shown that this fission process is in accordance with the knowledge from other fission reactions and thus is in the majority of cases a rather slow process. While until recently the intranuclear cascade evaporation calculations were in reasonable agreement with the experiments, some clear discrepancies have now appeared.

Acknowledgement

We appreciate the help in target preparation by A. Stolarz, K. Nacke, and P. Maier-Komor. We wish to thank J. Galin, M. Morjean, A. Peghaire, and B. Quednau for collaboration. The support by the Deutsche Forschungsgemeinschaft, by the Beschleunigerlaboratorium of the University and Technical University of Munich and by the Polish-German Scientific and Technical cooperation, Karlsruhe, is acknowledged.

[1] T. von Egidy, Nature 328, 773 (1987), J. Jastrzebski, P. Lubinsky, and A. Trzcinska, Acta Physica Polonica **B26,** 527 (1995).

[2] J. Jastrzebski, H. Daniel, T. von Egidy, A Grabowska, Y. S. Kim, W. Kurcewicz, P. Lubinski, G. Riepe, W. Schmid, A. Stolarz, and S. Wycech, Nucl. Phys. **A558,** 405c (1993).

[3] P. Lubinski, J. Jastrzebski, A. Grochulska, A. Stolarz, A. Trzcinska, W. Kurcewicz, F. J. Hartmann, W. Schmid, T. von Egidy, J. Skalski, R. Smolanczuk, S. Wycech, D. Hilscher, D. Polster, and H. Rossner, Phys. Rev. Lett **73,** 3199 (1994).

[4] P. Lubinski, A. Grochulska, J. Jastrzebski, W. Kurcewicz, J. Skalski, R. Smolanczuk, A. Stolarz, A. Trzcinska, S. Wycech, T. von Egidy, F. J. Hartmann, D. Hilscher, D. Polster, H. Rossner, and W. Schmid, in Raport Roczny 1994, Uniwersytet Warszawski, Srodowiskowe Laboratorium Ciezkich Jonow, Warsaw 1995, p. 53.

[5] S. Wycech, F. J. Hartmann, H. Daniel, W. Kanert, H. S. Plendl, T. von Egidy, J. J. Reidy, M. Nicholas, L. A. Redmond, H. Koch, A. Kreissl, H. Poth, and D. Rohmann, Nucl. Phys. **A561,** 607 (1993).

[6] P. Hofmann, A. S. Iljinov, Y. S. Kim, M. V. Mebel, H. Daniel, P. David, T. von Egidy, T. Haninger, F. J. Hartmann, J. Jastrzebski, W. Kurcewicz, J. Lieb, H. Machner, H. S. Plendl, G. Riepe, B. Wright, and K. Ziock, Phys. Rev. **C49,** 2555 (1994).

[7] A. Trzcinska, K. Gulda, J. Jastrzebski, W. Kurcewicz, P. Lubinski, L. Pienkowski, T. von Egidy, J. Galin, F. J. Hartmann, D. Hilscher. W. Schmid, and S. Schmid, Raport Roczny 1994, Uniwersytet Warszawski, Srodowiskowe Laboratorium Ciezkich Jonow, Warsaw 1995, p. 57.

[8] S. B. Kaufmann and E. P. Steinberg, Phys. Rev. **C22,** 167 (1980).

[9] D. H. Hinde, D. Hilscher, and H. Rossner, Nucl. Phys. **A 502,** 497c (1989).
[10] D. Hilscher and H. Rossner, Ann. Phys. Fr. **17,** 471 (1992).
[11] D. J. Hinde, H. Ogata, M. Tanaka, T. Shimoda, N. Takahashi, A. Shinohara, S. Wakamatsu, and H. Okamura, Phys. Rev. **C 39** 2268 (1989).
[12] Z. Fraenkel, A. Breskin, R. Chechik, S. Wald, R. Abegg, H. W. Fielding, P. Kitching, S. T. Lam, G. C. Neilson, and W. C. Olsen, J. Uegaki, Phys. Rev. **C41,** 1050 (1990).
[13] D. J. Hinde, D. Hilscher, H. Rossner, B. Gebauer, M. Lehmann, and M. Wilper, Phys. Rev. **C45**, 1129 (1992).
[14] A. S. Iljinov, V. I. Nazaruk, and S. E. Chigrinov, Nucl. Phys. **A 382,** 378 (1982).
[15] W. Schmid, P. Baumann, H. Daniel, T. von Egidy, F. J. Hartmann, P. Hofmann, Y. S. Kim, H. H. Schmidt, A. S. Iljinov, M. V. Mebel, D. Hilscher, D. Polster, H. Rossner, Nucl. Phys. **A 569,** 689 (1994).
[16] D. I. Ivanov, A. S. Iljinov, M. V. Mebel, V. G. Nedorezov, A. S. Sudov, A. A. Turinge, T. von Egidy, S. Schmid, W. Schmid, H. Rossner, and J. Eades, Z. Physik **A 352,** 191 (1995).
[17] W. Bohne, H. Morgenstern, and P. Figura, HMI-Jahresbericht 1991, p. 92.
[18] J. Galin and U. Jahnke, J. Phys. **G 20,** 1105 (1994).
[19] J. P. Bocquet, F. Malek, H. Nifenecker, M. Rey-Campagnolle, M. Maurel, E. Monnand, C. Perrin, C. Ristori, G. Ericsson, T. Johansson, G. Tibell, S. Polikanov, T. Krogulski, and J. Mougey, Z. Phys. **A 342,** 183 (1992).
[20] H. J. Krappe, J. R. Nix, and A. S. Sierk, Phys. Rev. **C 20,** 992 (1979).